

Supplementary

Collision-Induced Dissociation Mechanism of Sodiated Hex-HexNAc Disaccharides

Hock-Seng Nguan¹, Shang-Ting Tsai^{1,2}, Chia Yen Liew^{1,3,4}, and Chi-kung Ni^{1,5*}

¹ Institute of Atomic and Molecular Sciences, Academia Sinica, P. O. Box 23-166, Taipei 10617, Taiwan

² Current address: Department of Applied Chemistry, National Chiayi University, Chiayi City 600355, Taiwan

³ International Graduate Program of Molecular Science and Technology, National Taiwan University (NTU-MST), Taipei 10617, Taiwan

⁴ Molecular Science and Technology (MST), Taiwan International Graduate Program (TIGP), Academia Sinica, Taipei 10617, Taiwan

⁵ Department of Chemistry, National Tsing Hua University, Hsinchu 30013, Taiwan.

*Email address: ckni@po.iams.sinica.edu.tw

Calculation procedure	β Gal-13- α GalNAc	β Gal-13- β GalNAc	β Glc-13- α GlcNAc	β Glc-13- β GlcNAc	β Gal-14- α GalNAc	β Gal-14- β GalNAc	β Glc-14- α GlcNAc	β Glc-14- β GlcNAc
Multi-walker well-tempered metadynamics MD simulations to generate initial state structures.	150,000	150,000	150,000	150,000	150,000	150,000	150,000	150,000
↓								
Structural screening to remove duplicated structures	98,019	99,848	97,496	95,179	117,000	117,419	107,073	94,561
↓								
DFTB structural optimization	98,019	99,848	97,496	95,179	117,000	117,419	107,073	94,561
↓								
Structural screening to remove duplicated structures	19,009	26,269	8,569	16,176	42,620	67,974	19,815	29,790
↓								
Selection according to TS candidate criteria	10,723	13,297	6,834	10,787	20,229	21,856	12,393	14,166
↓								
DFT/B3LYP/6-31+G(d)+D3 optimization	10,723	13,297	6,834	10,787	20,229	21,856	12,393	14,166
↓								
Structural screening to remove duplicated structures	2,140	2,668	1,014	1,286	1,897	2,463	1,384	1,612
↓								
NEB calculations	2,305	1,404	1,317	1,696	3,039	5,164	2,048	1,874
↓								
TS optimization with DFT/ M06-2X/6-31+G(d,p)	1,030	1,074	904	1,165	1,235	3,592	1,630	1,379
↓								
TS confirmed by IRC with DFT/ M06-2X/6-31+G(d,p)	324	185	246	251	314	651	446	234

Figure S1. Calculation procedure and number of conformers in each calculation stage for the eight disaccharides Hex-HexNAc of sodium adducts.

Reactions	Number of TSs found							
	β Gal-13- α GalNAc	β Gal-13- β GalNAc	β Glc-13- α GlcNAc	β Glc-13- β GlcNAc	β Gal-14- α GalNAc	β Gal-14- β GalNAc	β Glc-14- α GlcNAc	β Glc-14- β GlcNAc
B ₁ -Y ₁	10	13	27	32	22	15	19	3
C ₁ -Z ₁ type1	52	54	14	22	219	309	136	73
C ₁ -Z ₁ type2	13	27	3	3	17	29	10	12
Dehydration	30	13	7	13	4	41	10	41
Ring-opening	219	78	195	181	52	257	271	105

Table S1. The number of transition state structures found for the eight disaccharides Hex-HexNAc of sodium adducts according to types of fragmentation reaction.

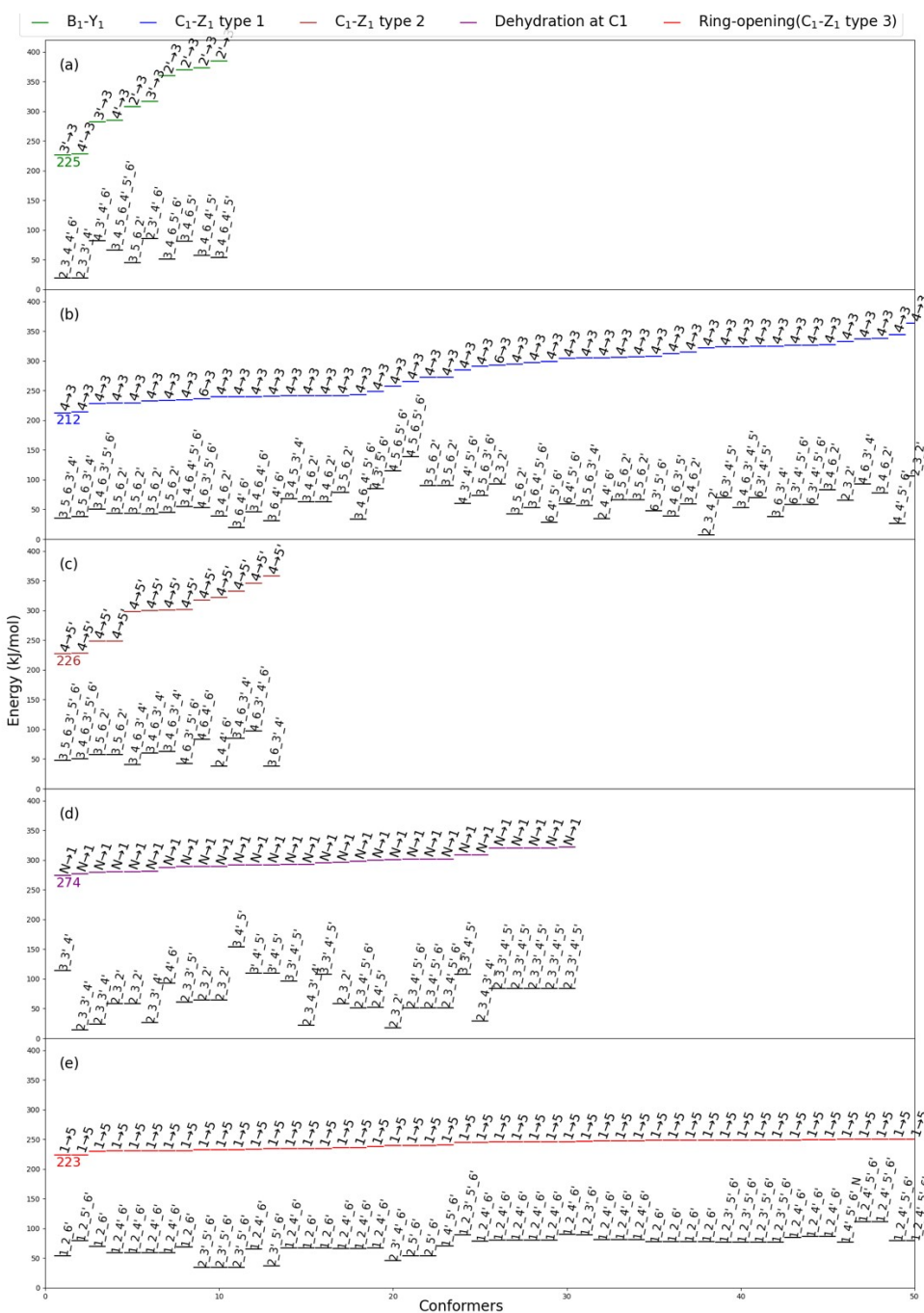


Figure S2. Calculated energies of TSs and reactants of sodiated β -Gal-(1 \rightarrow 3)- α -GalNAc using the DFT/M06-2X method. Up to 50 lowest of them are displayed. The energy is relative to the energy of the global minimum structure. The green, blue, brown, purple, and red dashes represent the TS energies of different reactions. Right above the TS dashes, the H-atom transfer that responsible for the TS is illustrated, with notations X \rightarrow Y indicates the H-atom transfer from X(O_D) to Y(O_A) atoms. The black dashes right below each TS dashes represent the energies of the reactant states leading to the TSs, where the series of numbers represents the numberings of O atoms binding to sodium ions.

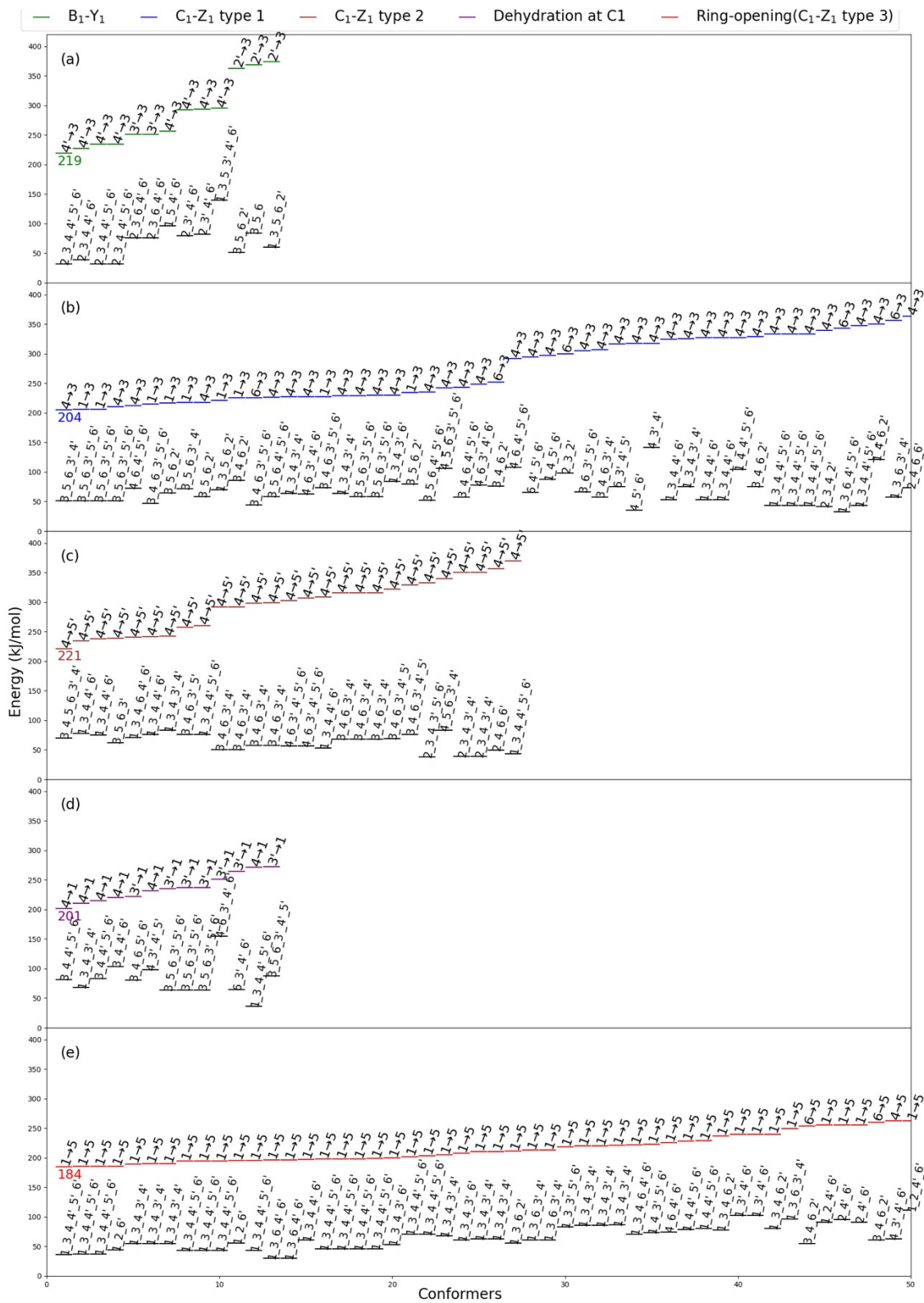


Figure S3. Calculated energies of TSs and reactants of sodiated β -Gal-(1 \rightarrow 3)- β -GalNAc using the DFT/M06-2X method. Up to 50 lowest of them are displayed.

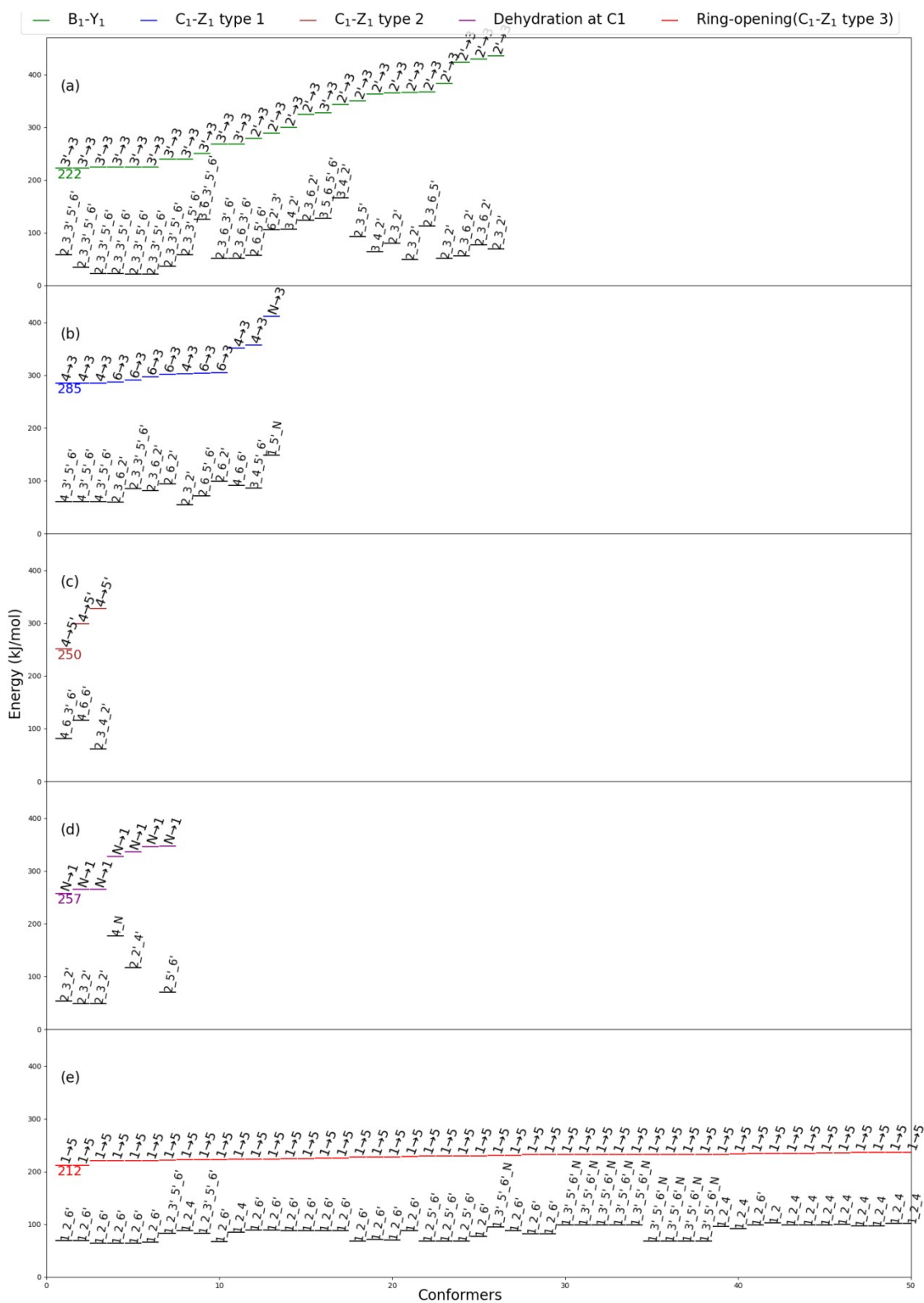


Figure S4. Calculated energies of TSs and reactants of sodiated β -Glc-(1 \rightarrow 3)- α -GlcNAc using the DFT/M06-2X method. Up to 50 lowest of them are displayed.

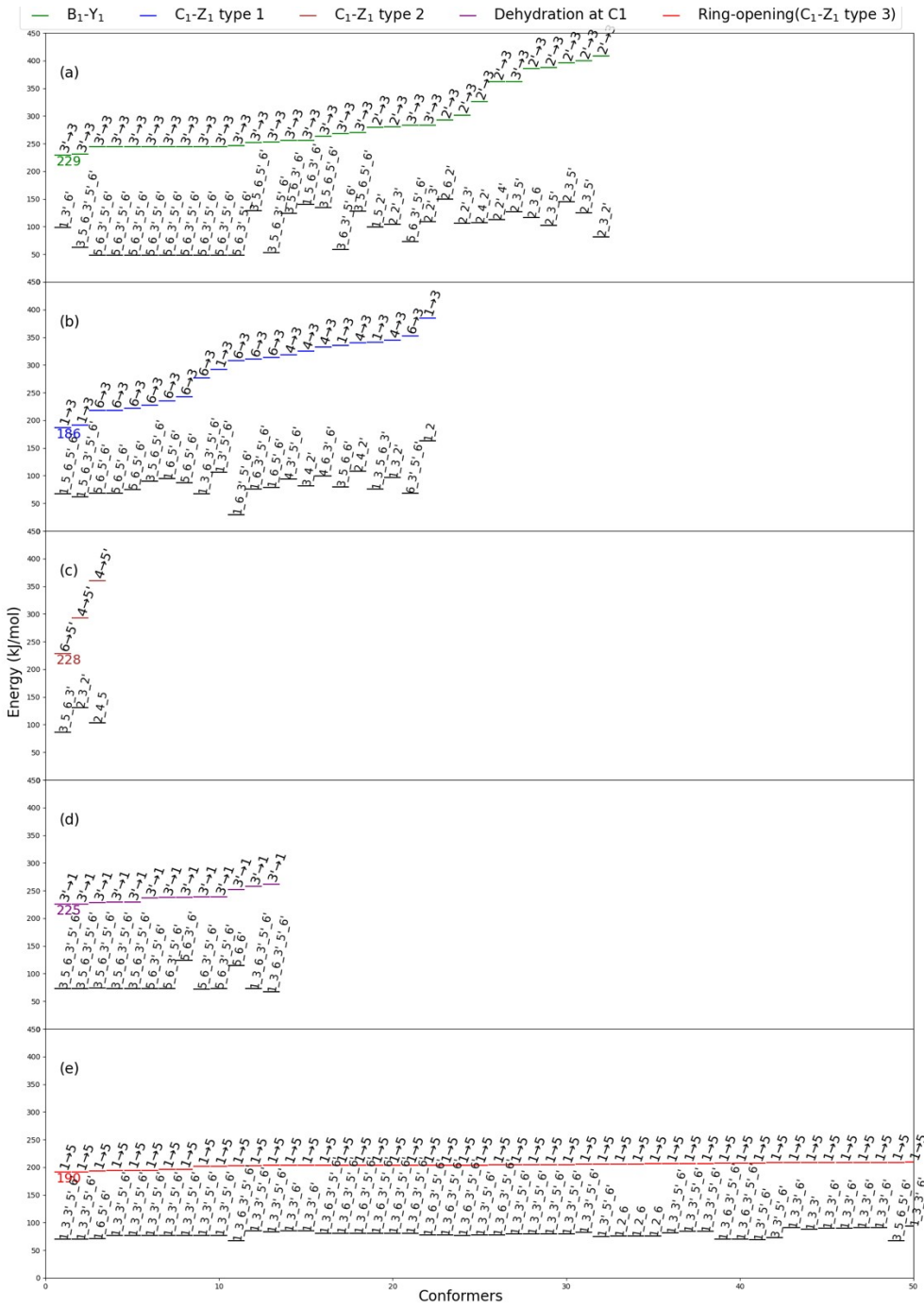


Figure S5. Calculated energies of TSs and reactants of sodiated β -Glc-(1 \rightarrow 3)- β -GlcNAc using the DFT/M06-2X method. Up to 50 lowest of them are displayed.

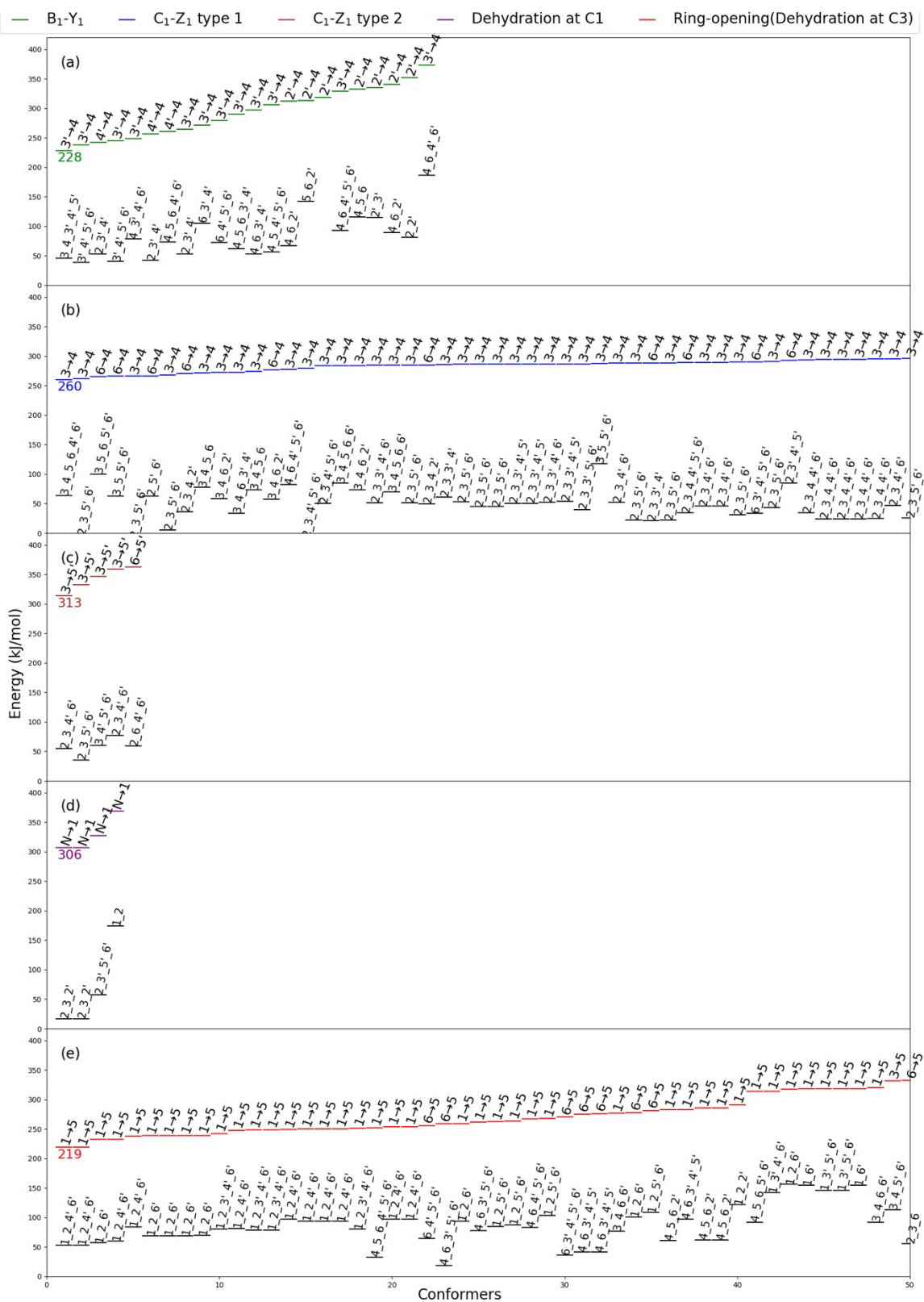


Figure S6. Calculated energies of TSs and reactants of sodiated β -Gal-(1 \rightarrow 4)- α -GalNAc using the DFT/M06-2X method. Up to 50 lowest of them are displayed.

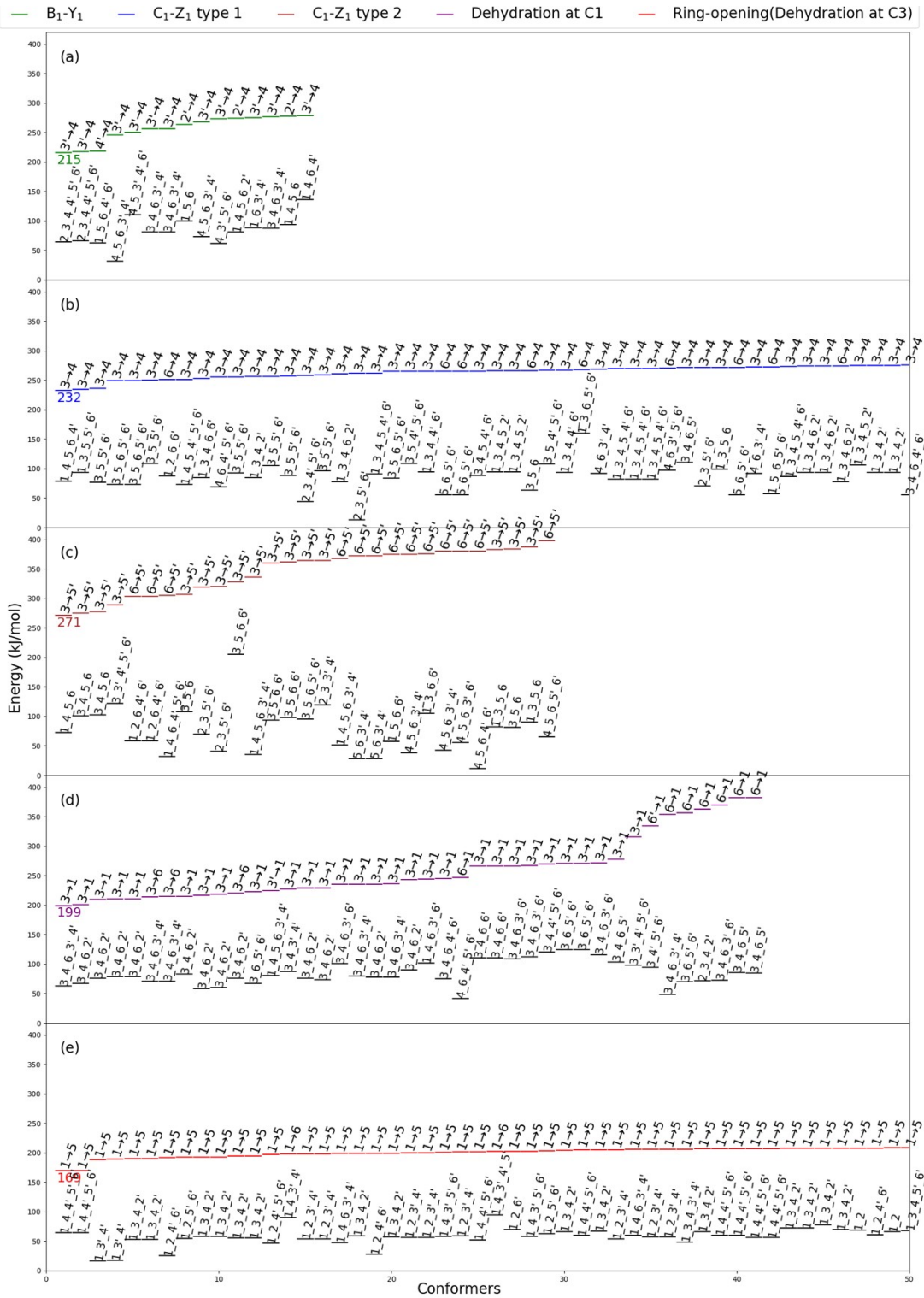


Figure S7. Calculated energies of TSs and reactants of sodiated β -Gal-(1 \rightarrow 4)- β -GalNAc using the DFT/M06-2X method. Up to 50 lowest of them are displayed.

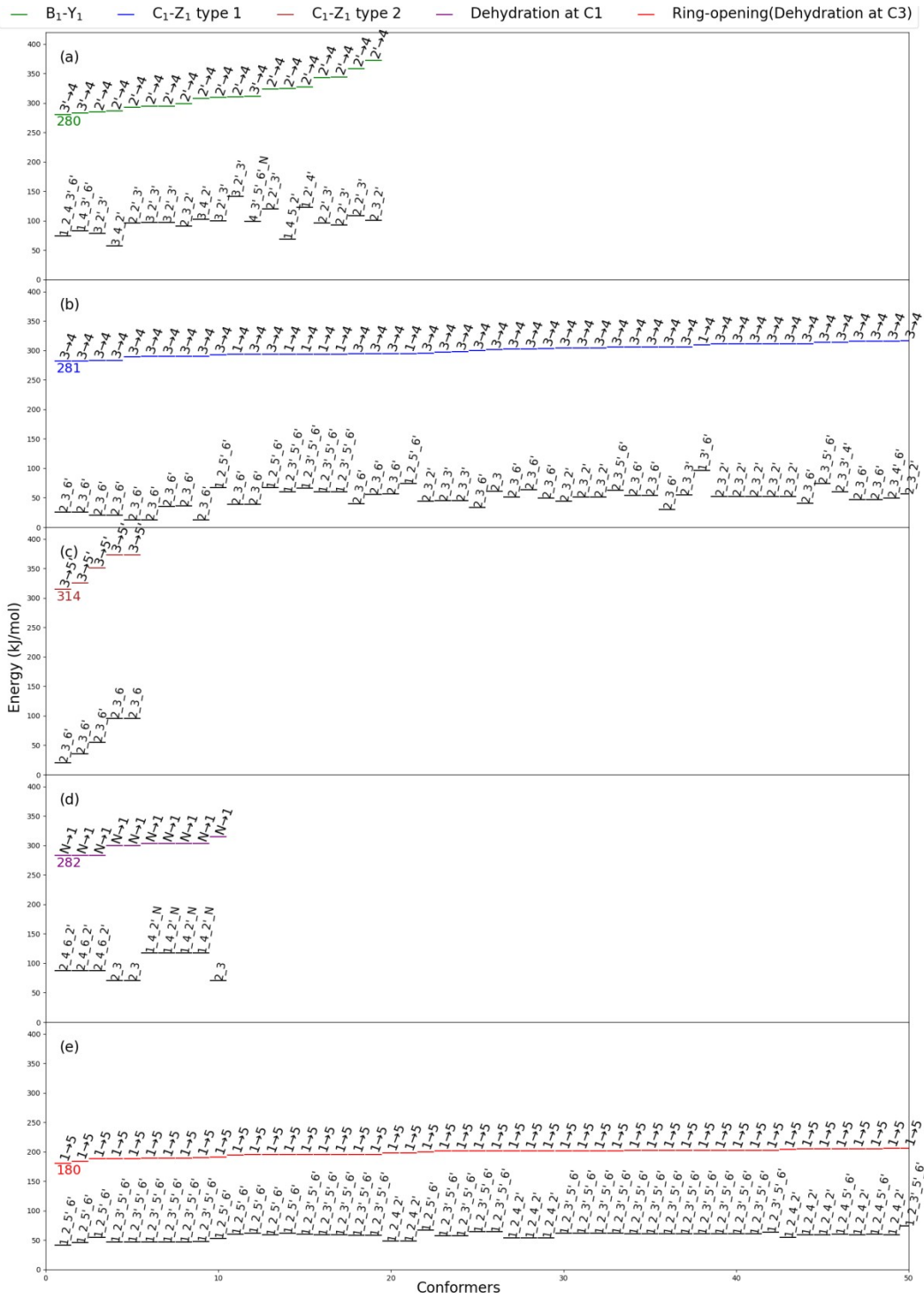


Figure S8. Calculated energies of TSs and reactants of sodiated β -Glc-(1 \rightarrow 4)- α -GlcNAc using the DFT/M06-2X method. Up to 50 lowest of them are displayed.

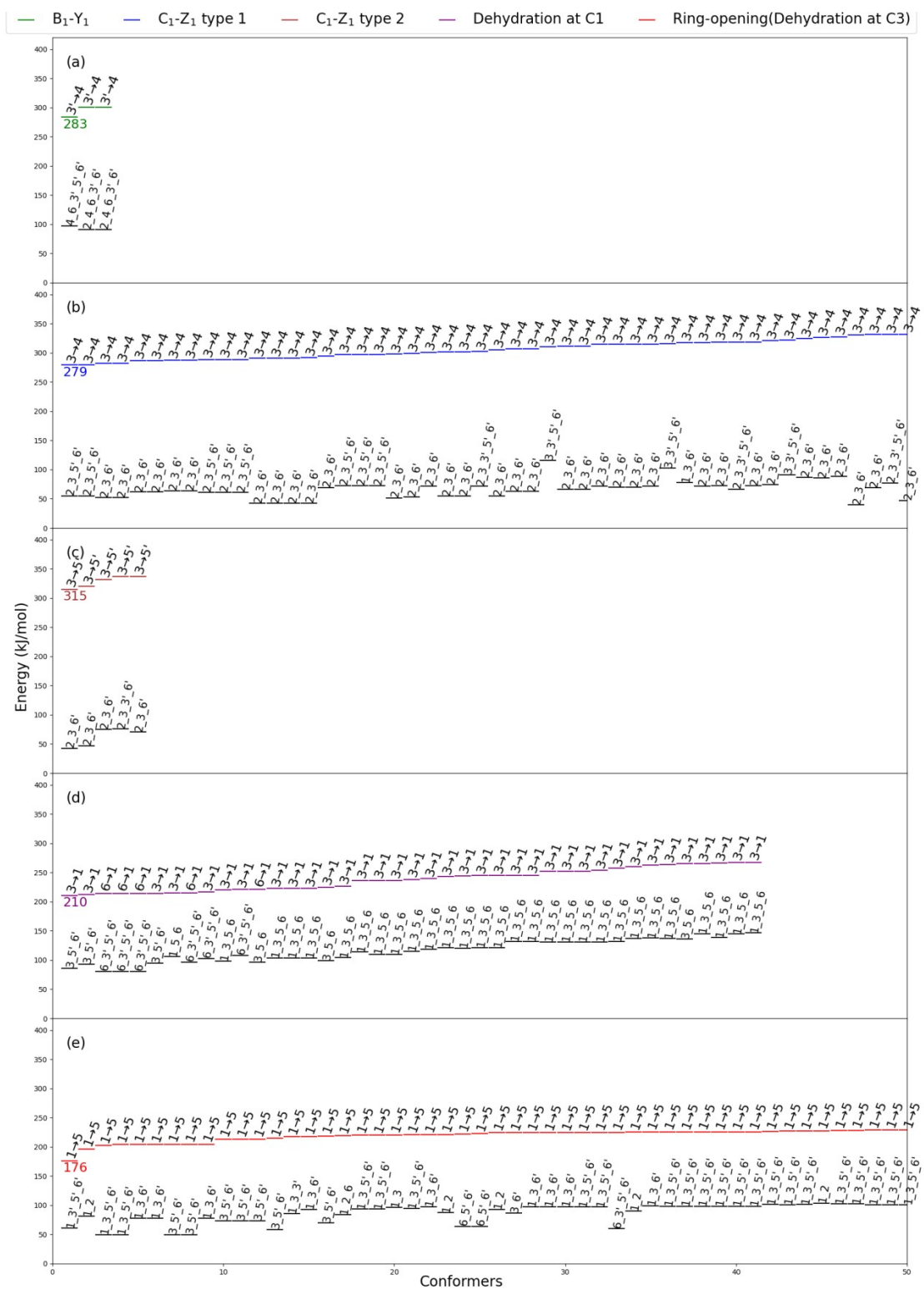
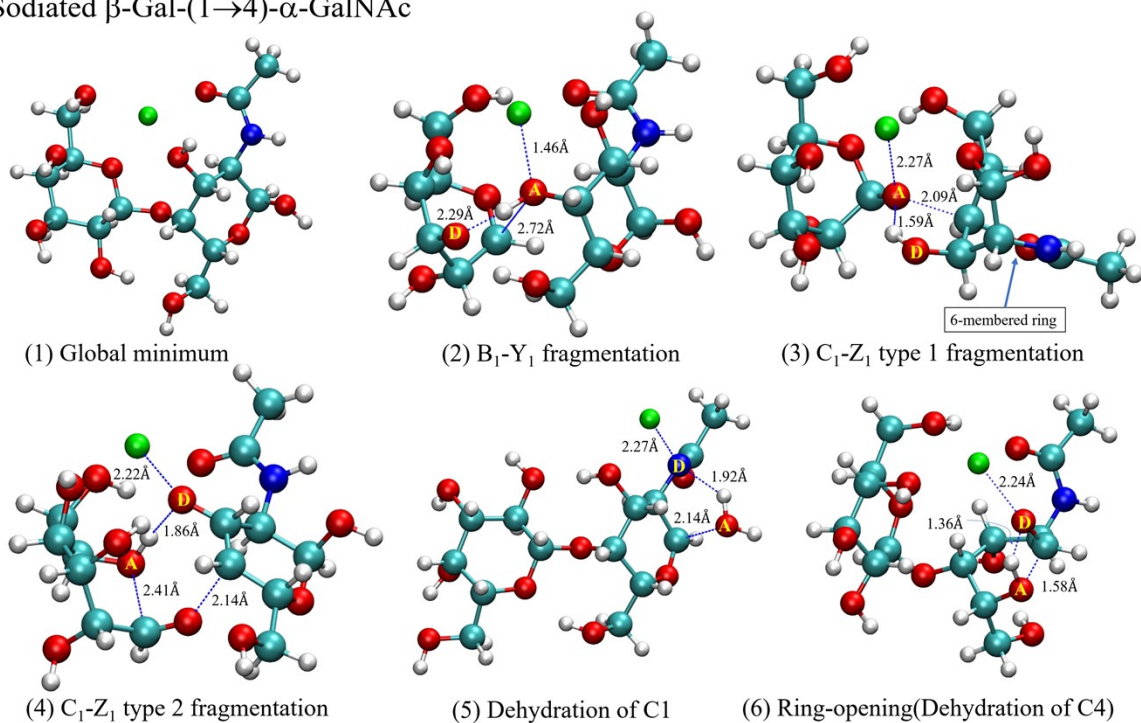


Figure S9. Calculated energies of TSs and reactants of sodiated β-Glc-(1→4)-β-GlcNAc using the DFT/M06-2X method. Up to 50 lowest of them are displayed.

TS structures of β -Gal-(1 \rightarrow 4)-GalNAc

The structures of global minimum and TSs of various reactions for β -Gal-(1 \rightarrow 4)- α -GalNAc and β -Gal-(1 \rightarrow 4)- β -GalNAc obtained from the calculations are displayed Fig. S10(a) and (b), respectively. The lowest TS structure of B₁-Y₁ fragmentation for β -Gal-(1 \rightarrow 4)- α -GalNAc [Fig. S10(a2)] suggests the process of C1'-O4 cleavage is promoted by the Na⁺-O4 binding and H is transferred from a nearby H-atom of O3' to O4. The same mechanism is found for the lowest TS of the B₁-Y₁ fragmentation for β -Gal-(1 \rightarrow 4)- β -GalNAc [Fig. S10(b2)]. A similar mechanism is expected in both cases since the B₁-Y₁ fragmentation is primarily influenced by the geometry of the sugar at the non-reducing end, which is β -Gal for both two disaccharides.

(a) Sodiated β -Gal-(1 \rightarrow 4)- α -GalNAc



(b) Sodiated β -Gal-(1 \rightarrow 4)- β -GalNAc

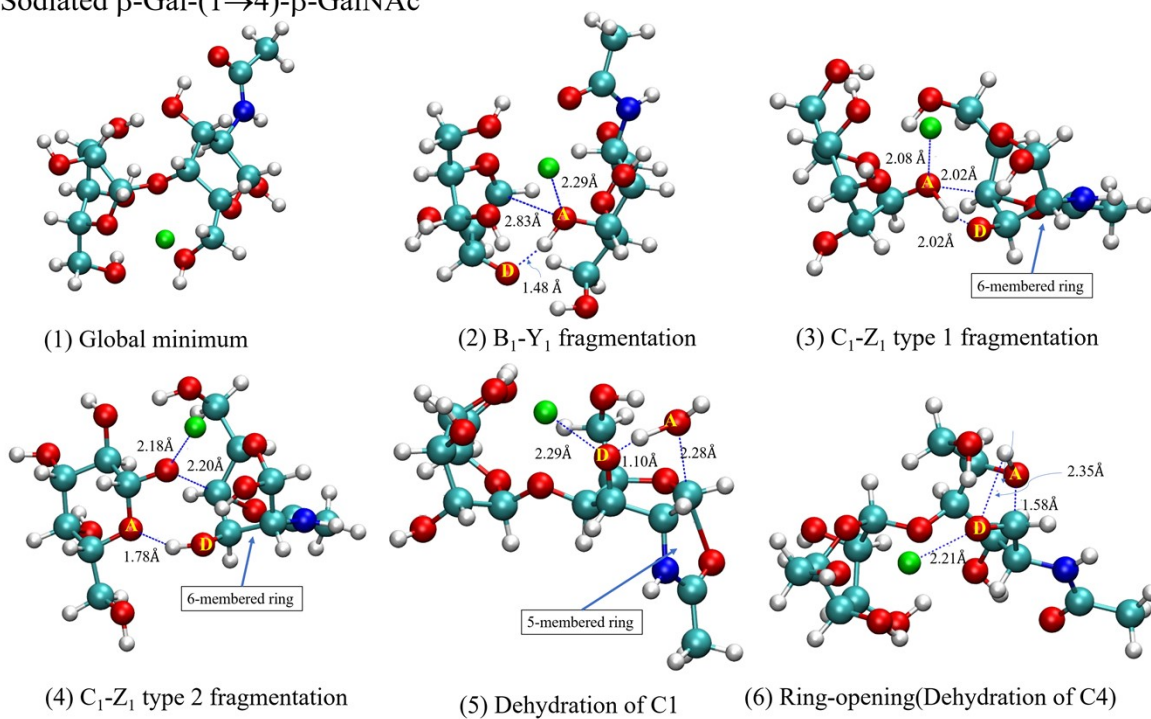


Figure S10. Geometries of global minimum and TS of various reactions for sodiated (a) β -Gal-(1 \rightarrow 4)- α -GalNAc and (b) β -Gal-(1 \rightarrow 4)- β -GalNAc obtained through DFT/M06-2X calculations. O atoms labeled as D and A are H-

atom donors and acceptors, respectively. Cyan, red, white, blue, and green balls represent carbon, oxygen, hydrogen, nitrogen and sodium atoms, respectively.

For type 1 C_1-Z_1 fragmentation, the lowest TS structures for β -Gal-(1 \rightarrow 4)- α -GalNAc [Fig. S10(a3)] and β -Gal-(1 \rightarrow 4)- β -GalNAc [Fig. S10(a3)] suggest that the O4-C4 cleavage is promoted by the Na^+ -O4 binding and H atom is transferred from a nearby H-atom of O3, and the formation of a six-membered ring through the covalent bond established between the O-atom of NAc group and C4. Although this mechanism is similar to that of their 1-3 linkage, unlike the 1-3 linked Gal-GalNAc which the TS energy of type 1 C_1-Z_1 fragmentation is lower than that of B_1-Y_1 fragmentation, the TS energy of type 1 C_1-Z_1 fragmentation is higher than that of B_1-Y_1 fragmentation in 1-4 linked Gal-GalNAc.

For type 2 C_1-Z_1 fragmentation, the lowest TS structure of both β -Gal-(1 \rightarrow 4)- α -GalNAc [Fig. S10(a4)] and β -Gal-(1 \rightarrow 4)- β -GalNAc [Fig. S10(b4)] are the results of H-atom transfer from O3 to O5'. However, in the case of β -Gal-(1 \rightarrow 4)- α -GalNAc, Na^+ -O3 bond promotes the H-atom transfer, while for β -Gal-(1 \rightarrow 4)- β -GalNAc Na^+ -O4 bond promotes the C4-O4 bond cleavage. Formation of a six-membered ring through a covalent bond formed between O atom of NAc group with C4 can be found only in the TS structure of β -Gal-(1 \rightarrow 4)- β -GalNAc

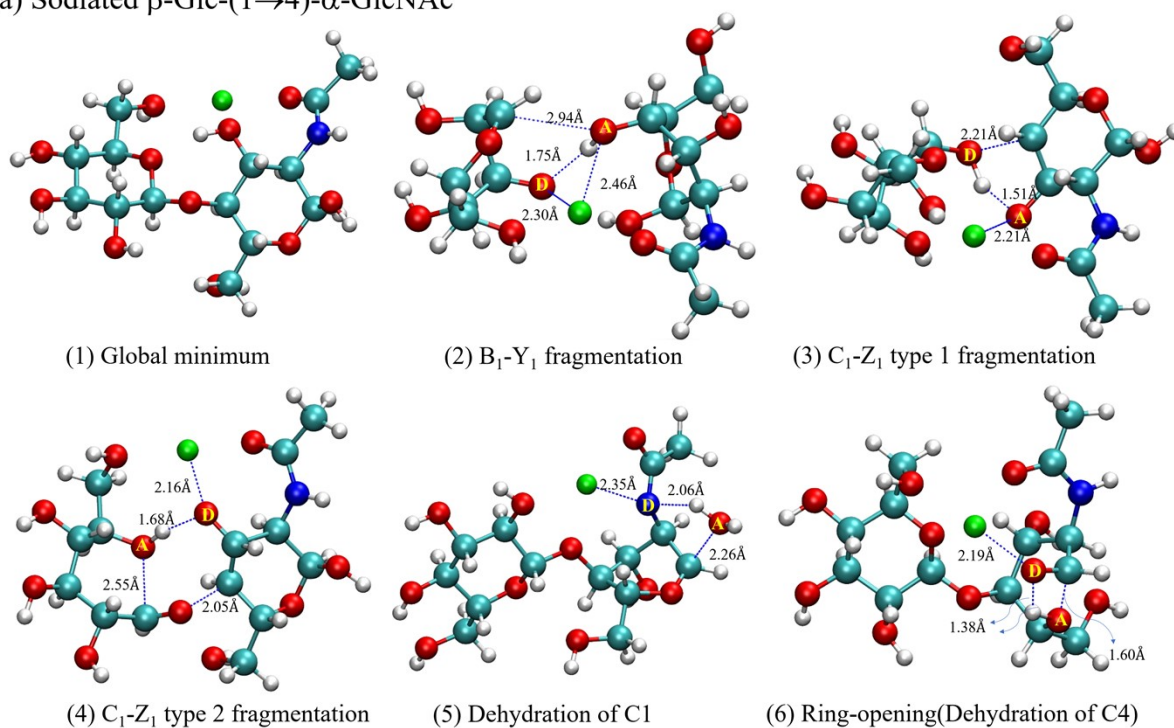
Similar to the β -Gal-GalNAc with 1-3 linkage, between β -Gal-(1 \rightarrow 4)- α -GalNAc and β -Gal-(1 \rightarrow 4)- β -GalNAc, the significant difference found in TS energies of dehydration of C1 and that of ring-opening reaction can be attributed to the hydroxyl group distribution on different sides of their GalNAc ring plane. For β -Gal-(1 \rightarrow 4)- α -GalNAc, only NAc group is at the same side of the ring plane as O1. Hence, dehydration at C1 that involves H-atom transfer from N to O1 [Fig. S10(a5)] results in high energy barrier due to the low acidity of N-H group. For β -Gal-(1 \rightarrow 4)- β -GalNAc, O1, O3 and O6 are on the same side of the plane. Its dehydration at C1 [Fig. S10(b5)] involves H-atom transfer from O3 to O1, which barrier is low due to the high acidity of O-H group. Furthermore, a five-membered ring is formed by the formation of a covalent bond between the O atom (from NAc group) and C1 in β -Gal-(1 \rightarrow 4)- β -GalNAc, which further reduces the reaction barrier.

The structures of the lowest ring-opening reaction TS of both sodiated β -Gal-(1 \rightarrow 4)- α -GalNAc [Fig. S10(a6)] and β -Gal-(1 \rightarrow 4)- β -GalNAc [Fig. S10(b6)] show the H-atom transfer is from O1 to O5. The lower ring-opening reaction TS for β -Gal-(1 \rightarrow 4)- β -GalNAc can be rationalized by the higher number of Na⁺-O binding in the reactant states compared to that of β -Gal-(1 \rightarrow 4)- α -GalNAc .

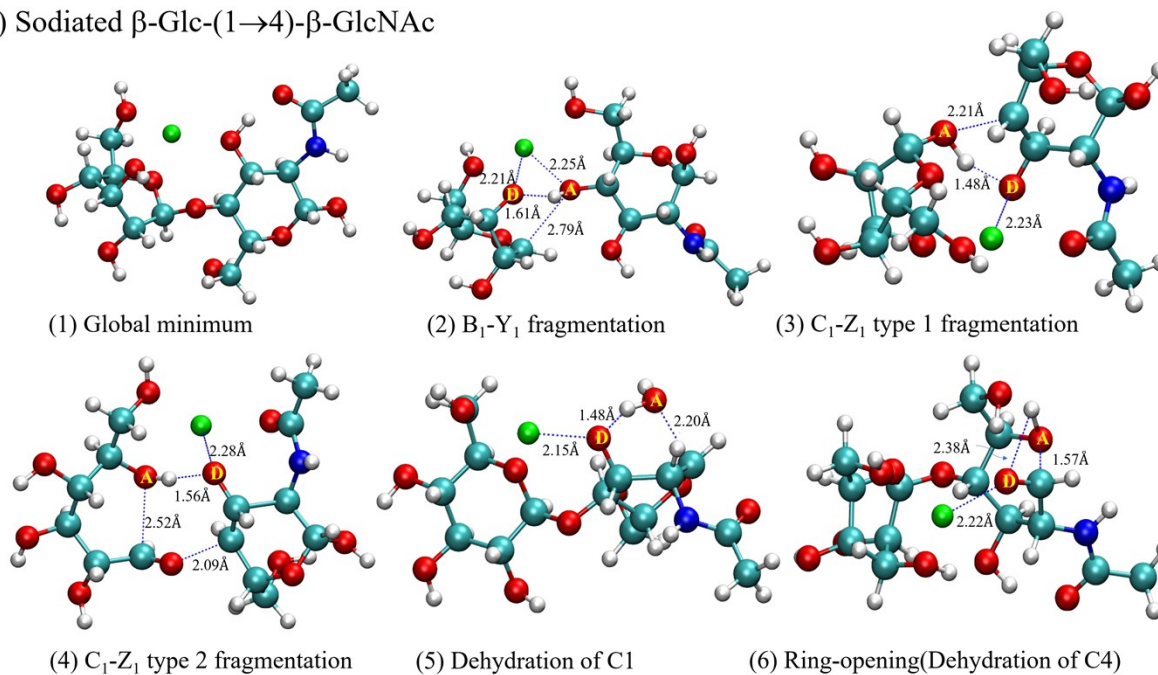
TS structures of β -Glc-(1 \rightarrow 4)-GlcNAc

The structures of the global minimum and the lowest TS of different reaction for β -Glc-(1 \rightarrow 4)- α -GlcNAc and β -Glc-(1 \rightarrow 4)- β -GlcNAc are given in Fig. S11(a) and (b), respectively. The lowest TSs of B₁-Y₁ fragmentation mechanism of β -Glc-(1 \rightarrow 4)- α -GlcNAc [Fig. S11(a2)] and β -Glc-(1 \rightarrow 4)- β -GlcNAc [Fig. S11(b2)] are found to be similar to that of β -Gal-(1 \rightarrow 4)- α -GalNAc and β -Gal-(1 \rightarrow 4)- β -GalNAc, where Na⁺ binds to O4 to promote the C1'-O4 cleavage and a nearby H-atom from O3' transfers to O4. . However, the reaction barrier in this case is higher for sodiated β -Glc-(1 \rightarrow 4)- α -GlcNAc and β -Glc-(1 \rightarrow 4)- β -GlcNAc compared to that of the of β -Gal-(1 \rightarrow 4)- α -GalNAc and β -Gal-(1 \rightarrow 4)- β -GalNAc because O3' and O4 (O1') are at different sides of the sugar-ring plane in β -Glc.

(a) Sodiated β -Glc-(1 \rightarrow 4)- α -GlcNAc



(b) Sodiated β -Glc-(1 \rightarrow 4)- β -GlcNAc



Fig

ure S11. Geometries of global minimum and TS of various reactions for sodiated (a) β -Glc-(1 \rightarrow 4)- α -GlcNAc and (b) β -Glc-(1 \rightarrow 4)- β -GlcNAc obtained through DFT/M06-2X calculations. O atoms labeled as D and A are H-atom donors and acceptors, respectively. Cyan, red, white, blue, and green balls represent carbon, oxygen, hydrogen, nitrogen and sodium atoms, respectively.

In type 1 C_1-Z_1 fragmentation, both β -Glc-(1 \rightarrow 4)- α -GlcNAc [Fig. S11(a3)] and β -Glc-(1 \rightarrow 4)- β -GlcNAc [Fig. S11(b3)] have the similar mechanism where the Na^+ binds to O3 and promotes the H-atom transfer from O3 to O4. Their TS energies are significantly higher compared to those of β -Gal-(1 \rightarrow 4)- α -GalNAc and β -Gal-(1 \rightarrow 4)- β -GalNAc, because of (1) O3 and O4 are on the opposite side of the β -GalNAc ring plane and (2) the NAc group does not form a six-membered ring. In type 2 C_1-Z_1 fragmentation, the mechanisms of both β -Glc-(1 \rightarrow 4)- α -GlcNAc [Fig. S11(a4)] and β -Glc-(1 \rightarrow 4)- β -GlcNAc [Fig. S11(b4)] involve the H-atom transfer from O3 to O5' and no six-membered ring is formed.

Analogous to β -Glc-(1 \rightarrow 3)-GlcNAc, the dehydration at C1 for β -Glc-(1 \rightarrow 4)- α -GlcNAc [Fig. S11(a5)] involves the H-atom transfer from N to O1, while for β -Glc-(1 \rightarrow 4)- β -GlcNAc [Fig. S11(b5)] the H-atom is transferred from O3 to O1. The most preferred ring-opening reaction mechanism for both β -Glc-(1 \rightarrow 4)- α -GlcNAc [Fig. S11(a6)] and β -Glc-(1 \rightarrow 4)- β -GlcNAc [Fig. S11(b6)] are the same, which involve the H-atom transfer from O1 to O5. The numbers of NAc and OH groups on each side of GlcNAc ring plane are the same for α -GlcNAc and β -GlcNAc, thus the difference in TS energy of ring-opening reaction is small.